Chapter 4
Non-Homogeneous Tension Profile

Abstract In this chapter, we will look at the influence of a skewed tension profile on the divergence instability of a travelling, thin elastic plate. The travelling plate is subjected to axial tension at the supports, but the tension distribution along the supports is not uniform. For the nonuniformity, we will use a linear distribution. First, we will perform a dynamic analysis of small time-harmonic vibrations, after which we will concentrate on the divergence instability problem. We will see that a small inhomogeneity in the applied tension may have a large effect on the divergence modes, and that inhomogeneity in the tension profile may significantly decrease the critical velocity of the plate.

4.1 Dynamic Analysis of Axially Moving Plates

Let a rectangular part of the plate

$$\Omega \equiv \left\{(x, y) \in \mathbb{R}^2 \mid 0 < x < \ell,\ -b < y < b\right\}$$

be travelling at a constant velocity V_0 in the x direction between two rollers located at $x = 0$ and $x = \ell$, where ℓ and b are prescribed parameters. See Fig. 4.1. Let the considered part of the band be represented as an isotropic elastic plate, having constant thickness h, Poisson ratio ν, Young modulus E and bending rigidity D. We will make some notes on the orthotropic case later.

The plate is subjected to in-plane distributed forces

$$g = g(y) = T_0 + T(y) \tag{4.1}$$

applied at the plate boundaries $x = 0$ and $x = \ell$, acting in the x direction. The constant $T_0 > 0$ and the function $T(y)$, characterizing non-homogeneous in-plane tension of the axially moving plate, are considered given. The sides of the plate

N. Banichuk et al., *Mechanics of Moving Materials*,
Solid Mechanics and Its Applications 207, DOI: 10.1007/978-3-319-01745-7_4,

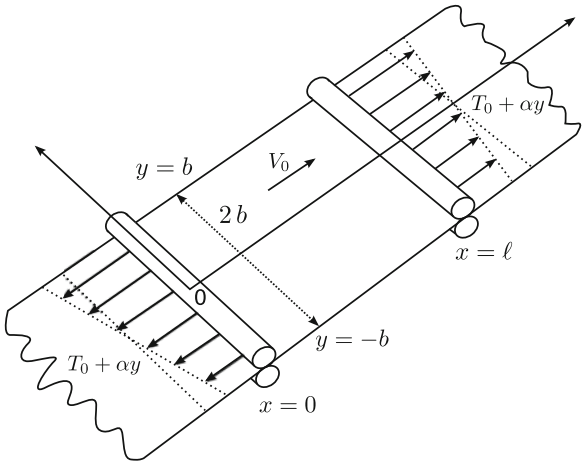

Fig. 4.1 Problem setup. A plate travelling at a constant velocity V_0 between two rollers placed at $x = 0$ and $x = \ell$. The tension profile is non-homogeneous and the tension is positive everywhere. (Reproduced from Banichuk et al. 2013)

$\{x = 0,\ -b \le y \le b\}$ and $\{x = \ell,\ -b \le y \le b\}$ are simply supported, and the sides $\{y = -b,\ 0 \le x \le \ell\}$ and $\{y = b,\ 0 \le x \le \ell\}$ are free of tractions.

4.2 Transverse Vibrations

The transverse displacement (out-of-plane deflection) of the travelling plate is described by the deflection function w, which depends on the space coordinates x and y, and time t. The differential equation for small transverse vibrations has the form

$$m\left(\frac{\partial^2 w}{\partial t^2} + 2V_0\frac{\partial^2 w}{\partial x\,\partial t} + V_0^2\frac{\partial^2 w}{\partial x^2}\right) = \mathcal{L}^{\mathrm{M}}(w) - \mathcal{L}^{\mathrm{B}}(w)\ , \qquad \text{in } \Omega\ . \tag{4.2}$$

The left-hand side in (4.2) contains three terms, respectively representing a local acceleration, a Coriolis acceleration and a centripetal acceleration. The membrane operator $\mathcal{L}^{\mathrm{M}}$ on the right-hand side of Eq. (4.2) is

$$\mathcal{L}^{\mathrm{M}}(w) = T_{xx}\frac{\partial^2 w}{\partial x^2} + 2\,T_{xy}\frac{\partial^2 w}{\partial x\,\partial y} + T_{yy}\frac{\partial^2 w}{\partial y^2}\ . \tag{4.3}$$

The coefficients T_{xx}, T_{xy}, T_{yy} of the linear operator $\mathcal{L}^{\mathrm{M}}$ are related to the corresponding in-plane stresses σ_{xx}, σ_{xy} and σ_{yy} by the expressions

$$T_{ij} = h\sigma_{ij}\ .$$

The linear bending operator $\mathcal{L}^{\mathrm{B}}$ is given by the expression

$$\mathcal{L}^{\mathrm{B}}(w) = D\Delta^2 w = D\left(\frac{\partial^4 w}{\partial x^4} + 2\frac{\partial^4 w}{\partial x^2 \partial y^2} + \frac{\partial^4 w}{\partial y^4}\right) \tag{4.4}$$

in the case of an isotropic elastic plate.

Boundary conditions for the deflection function w, corresponding to the simply supported boundaries and the free boundaries, can be written in the following form (see, e.g., Timoshenko and Woinowsky-Krieger 1959)

$$(w)_{x=0,\,\ell} = 0\,, \qquad \left(\frac{\partial^2 w}{\partial x^2}\right)_{x=0,\,\ell} = 0\,, \qquad -b \le y \le b\,, \tag{4.5}$$

$$\left(\frac{\partial^2 w}{\partial y^2} + \nu\frac{\partial^2 w}{\partial x^2}\right)_{y=\pm b} = 0\,, \qquad 0 \le x \le \ell\,, \tag{4.6}$$

$$\left(\frac{\partial^3 w}{\partial y^3} + (2-\nu)\frac{\partial^3 w}{\partial x^2 \partial y}\right)_{y=\pm b} = 0\,, \qquad 0 \le x \le \ell. \tag{4.7}$$

We represent the in-plane tensions T_{xx}, T_{xy} and T_{yy} with the help of the Airy stress function Υ:

$$T_{xx} = \frac{\partial^2 \Upsilon}{\partial y^2}\,, \qquad T_{yy} = \frac{\partial^2 \Upsilon}{\partial x^2}\,, \qquad T_{xy} = -\frac{\partial^2 \Upsilon}{\partial x \partial y}. \tag{4.8}$$

In this case of an isotropic plate, the Airy stress function Υ satisfies the biharmonic equation (see (2.46) of Sect. 2.2)

$$\Delta^2 \Upsilon \equiv \frac{\partial^4 \Upsilon}{\partial x^4} + 2\frac{\partial^4 \Upsilon}{\partial x^2 \partial y^2} + \frac{\partial^4 \Upsilon}{\partial y^4} = 0. \tag{4.9}$$

In what follows, we will concentrate on a linear tension distribution. The boundary conditions for the tension are (2.29) and (2.30) of Sect. 2.2, repeated here for convenience:

$$T_{xx} = g(y)\,, \qquad T_{xy} = 0 \quad \text{at } x = 0,\ \ell, \quad -b \le y \le b\,,$$

$$T_{yy} = 0\,, \qquad T_{xy} = 0 \quad \text{at } y = \pm b, \quad 0 \le x \le \ell.$$

The boundary conditions satisfied by Υ, corresponding to (2.29) and (2.30) are

$$\left(\frac{\partial^2 \Upsilon}{\partial y^2}\right)_{x=0,\ell} = g(y)\,, \quad \left(\frac{\partial^2 \Upsilon}{\partial x \partial y}\right)_{x=0,\ell} = 0\,, \quad -b \le y \le b\,, \tag{4.10}$$

$$\left(\frac{\partial^2 \Upsilon}{\partial x^2}\right)_{y=\pm b} = 0\,, \quad \left(\frac{\partial^2 \Upsilon}{\partial x \partial y}\right)_{y=\pm b} = 0\,, \quad 0 \le x \le \ell. \tag{4.11}$$

Recall that the tensions expressed via the stress function Υ in (4.8) will satisfy the equilibrium of in-plane tensions for any function Υ that is smooth enough. The equilibrium equations are (2.28) of Sect. 2.2, repeated here for convenience:

$$\frac{\partial T_{xx}}{\partial x} + \frac{\partial T_{xy}}{\partial y} = 0\,, \quad \frac{\partial T_{xy}}{\partial x} + \frac{\partial T_{yy}}{\partial y} = 0.$$

Equation (4.9), which must be solved, expresses the condition of compatibility for the tensions.

In what follows, we will concentrate on a linear tension distribution, and use the rigorous solution of the boundary value problem (4.9–4.11) corresponding to the case that

$$g(y) = T_0 + \alpha y \equiv T_0 + T(y). \tag{4.12}$$

Here $\alpha > 0$ is a given constant that will be called the tension profile skew parameter. We have

$$\Upsilon(x, y) = T_0 \frac{y^2}{2} + \alpha \frac{y^3}{6} + c_1 x + c_2 y + c_0, \quad (x, y) \in \Omega\,. \tag{4.13}$$

Here c_0, c_1 and c_2 are arbitrary constants. The corresponding tensions will be

$$T_{xx}(x, y) = T_0 + \alpha y, \quad T_{xy}(x, y) = 0, \quad T_{yy}(x, y) = 0, \quad (x, y) \in \Omega\,. \tag{4.14}$$

In this case, the dynamic equation takes the form

$$\frac{\partial^2 w}{\partial t^2} + 2\,V_0 \frac{\partial^2 w}{\partial x \partial t} + (V_0^2 - C^2) \frac{\partial^2 w}{\partial x^2} - \frac{T(y)}{m} \frac{\partial^2 w}{\partial x^2}$$

$$+ \frac{D}{m} \left(\frac{\partial^4 w}{\partial x^4} + 2 \frac{\partial^4 w}{\partial x^2 \partial y^2} + \frac{\partial^4 w}{\partial y^4}\right) = 0, \quad (x, y) \in \Omega\,, \tag{4.15}$$

where

$$C = \sqrt{\frac{T_0}{m}}\,, \qquad \text{and} \qquad T(y) = \alpha y.$$

Following the approach of Bolotin (1963), let us represent the solution of the nonstationary boundary value problem for the partial differential equation (4.15) with the boundary conditions (4.5–4.7) using the time-harmonic trial function

$$w(x, y, t) = W(x, y)\, e^{st}\,, \qquad s = i\omega. \tag{4.16}$$

Here, ω is the frequency of the small transverse vibrations, and s is the stability exponent, which is a complex number. As was explained in Sect. 3.2, if s is purely imaginary, then the plate performs harmonic vibrations with a small amplitude, and its motion can be considered to be stable. If the real part of s becomes positive, then the transverse vibrations grow exponentially and, consequently, the behaviour of the plate is unstable. Using this (complex-valued) representation we will have

$$s^2 W + 2sV_0 \frac{\partial W}{\partial x} + \left(V_0^2 - C^2\right) \frac{\partial^2 W}{\partial x^2} - \frac{T(y)}{m} \frac{\partial^2 W}{\partial x^2} + \frac{D}{m} \triangle^2 W = 0 \,. \tag{4.17}$$

The boundary conditions for W follow from (4.5–4.7), by inserting (4.16). We obtain

$$(W)_{x=0,\ell} = 0 \,, \qquad \left(\frac{\partial^2 W}{\partial x^2}\right)_{x=0,\ell} = 0 \,, \qquad -b \le y \le b \,, \tag{4.18}$$

$$\left(\frac{\partial^2 W}{\partial y^2} + \nu \frac{\partial^2 W}{\partial x^2}\right)_{y=\pm b} = 0 \,, \qquad 0 \le x \le \ell \,, \tag{4.19}$$

$$\left(\frac{\partial^3 W}{\partial y^3} + (2-\nu) \frac{\partial^3 W}{\partial x^2 \partial y}\right)_{y=\pm b} = 0 \,, \qquad 0 \le x \le \ell. \tag{4.20}$$

Compare (3.16–3.18) and (3.20).

We multiply (4.17) by W and perform integration over the domain Ω to obtain

$$s^2 \int_\Omega W^2 \, \mathrm{d}\Omega + 2sV_0 \int_\Omega W \frac{\partial W}{\partial x} \, \mathrm{d}\Omega + (V_0^2 - C^2) \int_\Omega W \frac{\partial^2 W}{\partial x^2} \, \mathrm{d}\Omega$$

$$- \frac{T(y)}{m} \int_\Omega W \frac{\partial^2 W}{\partial x^2} \, \mathrm{d}\Omega + \frac{D}{m} \int_\Omega W \triangle^2 W \, \mathrm{d}\Omega = 0. \tag{4.21}$$

Using the boundary conditions (4.18–4.20) and performing integration by parts, we find the same result as in (3.11) and (3.12):

$$\begin{aligned} \int_\Omega W \frac{\partial W}{\partial x} \, \mathrm{d}\Omega &= \int_{-b}^{b} \int_0^\ell W \frac{\partial W}{\partial x} \, \mathrm{d}x \, \mathrm{d}y \\ &= \int_{-b}^{b} \left[\frac{W^2(\ell, y)}{2} - \frac{W^2(0, y)}{2} \right] \mathrm{d}y \\ &= 0 \,, \end{aligned}$$

$$\int_\Omega W \frac{\partial^2 W}{\partial x^2} \, \mathrm{d}\Omega = - \int_\Omega \left(\frac{\partial W}{\partial x}\right)^2 \, \mathrm{d}\Omega.$$

The non-homogeneous tension-related integral admits the following representation:

$$\int_{\Omega} yW\frac{\partial^2 W}{\partial x^2}\,\mathrm{d}\Omega = -\int_{\Omega} y\left(\frac{\partial W}{\partial x}\right)^2\,\mathrm{d}\Omega. \tag{4.22}$$

We have

$$s^2\int_{\Omega} W^2\,\mathrm{d}\Omega + (C^2 - V_0^2)\int_{\Omega}\left(\frac{\partial W}{\partial x}\right)^2\,\mathrm{d}\Omega$$

$$+\frac{\alpha}{m}\int_{\Omega} y\left(\frac{\partial W}{\partial x}\right)^2\,\mathrm{d}\Omega + \frac{D}{m}\int_{\Omega} W\triangle^2 W\,\mathrm{d}\Omega = 0. \tag{4.23}$$

Two special cases, from which it is possible to draw further conclusions, will be considered. First, let $\alpha = 0$ and $T_{xx}(x, y) = T_0$, i.e. one assumes homogeneous tension. In this case, as it was shown in Sect. 3.3.2, the following relation takes place:

$$\int_{\Omega} W\,\triangle^2 W\,\mathrm{d}\Omega = \int_{\Omega}(\triangle W)^2\,\mathrm{d}\Omega + 2\int_0^{\ell} Q_{y=b}\,\mathrm{d}x. \tag{4.24}$$

Above, the abbreviation

$$Q = W\,\frac{\partial}{\partial y}(\triangle W) - \triangle W\,\frac{\partial W}{\partial y} \tag{4.25}$$

has been used. Note that in (4.24) symmetry properties of the original partial differential equation were used to obtain this form of the Q integral. Consequently, one has

$$\omega^2 = -s^2 =$$

$$\frac{(C^2 - V_0^2)\int_{\Omega}\left(\frac{\partial W}{\partial x}\right)^2\mathrm{d}\Omega + \frac{D}{m}\left[\int_{\Omega}(\triangle W)^2\,\mathrm{d}\Omega + 2\int_0^{\ell} Q_{y=b}\,\mathrm{d}x\right]}{\int_{\Omega} W^2\,\mathrm{d}\Omega}. \tag{4.26}$$

At the critical velocity, as can be seen from (4.26), the following relation between the critical velocity and the divergence mode holds:

$$\left(V_0^{\mathrm{div}}\right)^2 = C^2 + \frac{D}{m}\frac{\int_{\Omega}(\triangle W)^2\,\mathrm{d}\Omega + 2\int_0^{\ell} Q_{y=b}\,\mathrm{d}x}{\int_{\Omega}\left(\frac{\partial W}{\partial x}\right)^2\mathrm{d}\Omega}. \tag{4.27}$$

In order to determine that $Q_{y=b} > 0$ at this point, one needs to use the solution from the corresponding static problem, described in the next section for the general case.

With that observation, we see that all integrals on the right side of (4.27) are positive, and it holds that

$$\left(V_0^{\text{div}}\right)^2 > C^2. \tag{4.28}$$

It follows from (4.27) that if the bending rigidity of the web is negligibly small, then

$$\left(V_{0\,\text{mem}}^{\text{div}}\right)^2 = C^2 = \frac{T_0}{m}. \tag{4.29}$$

In the one-dimensional case of axially travelling strings, this is a known result (see, e.g., Chang and Moretti 1991). From (4.29), we see that the same value of the critical velocity also applies to ideal membranes. The expression for $V_{0\,\text{mem}}^{\text{div}}$, (4.29), does not depend on W. Thus, for the special case of an ideal membrane under homogeneous tension, any combination of modes may occur at the critical velocity.

Consider now a second special case, where the bending rigidity of the axially moving plate is negligibly small, and the in-plane tension in the x direction is positive. Thus we avoid compression and wrinkling considerations. Illustration can be seen in Fig. 4.1. We assume that

$$D = 0\,, \qquad T_0 > \alpha\, b\,, \tag{4.30}$$

where the latter condition comes from the constraints

$$T_{xx}(x, y) = T_0 + \alpha\, y > 0 \qquad \text{and} \qquad y \geq -b. \tag{4.31}$$

In this case, the characteristic parameter s is evaluated as

$$\omega^2 = -s^2 = \frac{(C^2 - V_0^2)\int_\Omega \left(\frac{\partial W}{\partial x}\right)^2 \mathrm{d}\Omega + \frac{\alpha}{m}\int_\Omega y \left(\frac{\partial W}{\partial x}\right)^2 \mathrm{d}\Omega}{\int_\Omega W^2\,\mathrm{d}\Omega}. \tag{4.32}$$

If a steady-state solution (divergence) exists, it will occur at velocity

$$\left(V_0^{\text{div}}\right)^2 = C^2 + \frac{\alpha}{m}\frac{\int_\Omega y \left(\frac{\partial W}{\partial x}\right)^2 \mathrm{d}\Omega}{\int_\Omega \left(\frac{\partial W}{\partial x}\right)^2 \mathrm{d}\Omega}. \tag{4.33}$$

Let us assume that the divergence mode W is a real-valued function. Taking into account the expression in (4.33), and the fact that $y \geq -b$, we can estimate the divergence velocity (from below) as

$$\left(V_0^{\text{div}}\right)^2 \geq C^2 - \frac{\alpha b}{m} = \frac{T_0 - \alpha b}{m}. \tag{4.34}$$

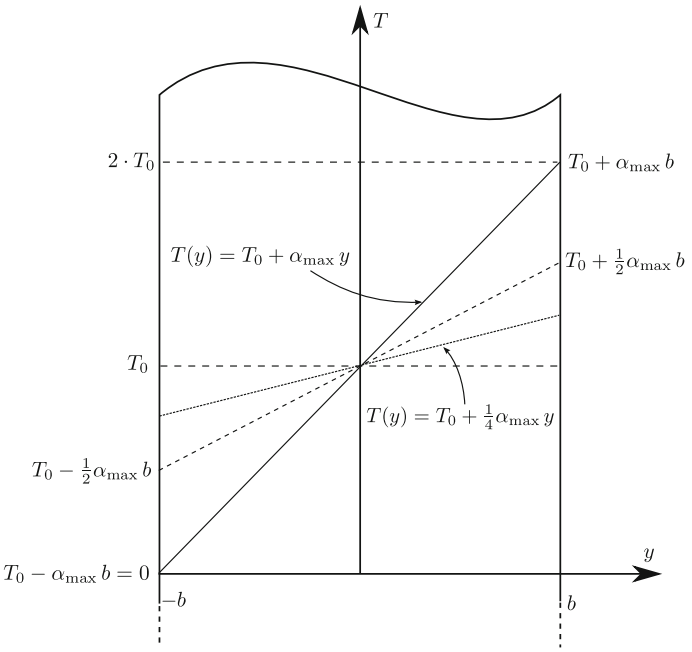

Fig. 4.2 The definition of α_{max}. It is the largest skew that retains $T(y) \geq 0$ across the whole domain, avoiding compression and wrinkling

We see from (4.34) that as long as the condition for T_0 in (4.30) is fulfilled, we have $(V_0^{\text{div}})^2 \geq 0$, i.e., the value of V_0^{div} is physically meaningful (Fig. 4.2).

4.3 Solution of Eigenvalue Problem

We will next consider the static instability of the travelling thin plate subjected to a linearly skewed tension profile. The treatment of the problem follows the same approach as in Sects. 3.4 and 3.5, where we analyzed the static instability of travelling isotropic and orthotropic plates under a under the assumption of a homogeneous tension profile.

4.3.1 Transformation to Ordinary Differential Equation

The stationary eigenvalue problem of elastic instability consists of finding a non-trivial solution (mode) and the corresponding minimal eigenvalue of the following boundary-value problem. Consider the steady-state equation, corresponding to $s = 0$ in the nonstationary problem in (4.17),

$$(V_0^2 - C^2)\frac{\partial^2 W}{\partial x^2} - \frac{T(y)}{m}\frac{\partial^2 W}{\partial x^2}$$

$$+ \frac{D}{m}\left(\frac{\partial^4 W}{\partial x^4} + 2\frac{\partial^4 W}{\partial x^2 \partial y^2} + \frac{\partial^4 W}{\partial y^4}\right) = 0\,, \quad (x, y) \in \Omega. \tag{4.35}$$

with the boundary conditions for W in (4.18–4.20). From the latter condition in (4.30), we obtain a constraint for α:

$$T(y) = \alpha y \qquad \text{and} \qquad \alpha < T_0/b. \tag{4.36}$$

To determine the minimal eigenvalue λ (see (3.39)) of the problem (4.18–4.20) and (4.35), and the corresponding eigenfunction, we apply the same representation as before:

$$W = W(x, y) = f\left(\frac{y}{b}\right)\sin\left(\frac{\pi x}{\ell}\right)\,, \tag{4.37}$$

where $f(y/b)$ is an unknown function. It follows from (4.37) that the divergence form (steady-state solution) W satisfies the boundary conditions (4.18).

As before, let us define the dimensionless quantities η and μ, given by (3.41),

$$\eta = \frac{y}{b}\,, \qquad \mu = \frac{\ell}{\pi b}\,, \tag{4.38}$$

and the eigenvalue λ as per (3.39),

$$\lambda = \gamma^2 = \frac{\ell^2}{\pi^2 D}\left(m V_0^2 - T_0\right). \tag{4.39}$$

By using the free-of-traction boundary conditions (4.19) and (4.20), the static equation (4.35) and the definition of W, (4.37), we obtain the following eigenvalue problem for the unknown function $f(\eta)$:

$$\mu^4 \frac{\mathrm{d}^4 f}{\mathrm{d}\eta^4} - 2\mu^2 \frac{\mathrm{d}^2 f}{\mathrm{d}\eta^2} + (1 - \lambda + \tilde{\alpha}\eta) f = 0\,, \quad -1 < \eta < 1\,, \tag{4.40}$$

where

$$\tilde{\alpha} = \frac{b\ell^2}{\pi^2 D}\alpha = \frac{b^3\mu^2}{D}\alpha. \tag{4.41}$$

Equation (4.40) is considered with the boundary conditions

$$\mu^2 \frac{\mathrm{d}^2 f}{\mathrm{d}\eta^2} - \nu f = 0\,, \quad \eta = \pm 1 \quad \text{and} \tag{4.42}$$

$$\mu^2 \frac{\mathrm{d}^3 f}{\mathrm{d}\eta^3} - (2-\nu)\,\frac{\mathrm{d} f}{\mathrm{d}\eta} = 0\,, \quad \eta = \pm 1\,, \tag{4.43}$$

which correspond to the free-of-traction boundary conditions of the original problem.

Equation (4.40) with the boundary conditions (4.42) and (4.43) constitutes a linear eigenvalue problem for f with polynomial coefficients.

For an orthotropic material, it is possible to use problem (4.40), (4.42–4.43) in a straightforward way by setting the orthotropic in-plane shear modulus G_{12} as the geometric average shear modulus

$$G_{\mathrm{H}} \equiv \frac{\sqrt{E_1 E_2}}{2\left(1+\sqrt{\nu_{12}\nu_{21}}\right)}\,,$$

and reducing the orthotropic problem into the isotropic one (see Timoshenko and Woinowsky-Krieger 1959).

Alternatively, if one wishes to keep G_{12} as an independent material parameter, which is more accurate for some materials, it is possible to derive the corresponding eigenvalue problem for the orthotropic plate following the same procedure that was used above for the isotropic plate (Fig. 4.3). Again, let the axial in-plane tension (4.1) take the form (4.12). As was noted, the value of α in (4.12) is constrained by (4.36). We have the following partial differential equation:

$$\left(m V_0^2 - T_0\right) \frac{\partial^2 W}{\partial x^2} - \frac{T(y)}{m}\,\frac{\partial^2 W}{\partial x^2} + D_0 \mathcal{L}_0(w) = 0\,, \tag{4.44}$$

where the differential operator $\mathcal{L}_0(w)$ is given by (3.4),

$$\mathcal{L}_0(w) = \frac{D_1}{D_0}\frac{\partial^4 w}{\partial x^4} + \frac{2D_3}{D_0}\frac{\partial^4 w}{\partial x^2 \partial y^2} + \frac{D_2}{D_0}\frac{\partial^4 w}{\partial y^4}\,,$$

and D_0 is an arbitrary normalization factor, which is convenient to take as $D_0 = D_1$. The coefficients D_j for $j = 1, 2, 3$ are the orthotropic bending rigidities

$$D_1 = \frac{h^3}{12} C_{11}\,, \quad D_2 = \frac{h^3}{12} C_{22}\,, \quad D_3 = \frac{h^3}{12}\left(C_{12} + 2\,C_{66}\right)\,,$$

which were already given as (2.18), Sect. 2.1.3 (or see Timoshenko and Woinowsky-Krieger 1959, chap. 11). The C_{ij} are the elastic moduli, (2.19).

The boundary conditions for W are given in (4.18–4.20). However, in the free edge boundary conditions (4.19) and (4.20), instead of the isotropic free boundary coefficients ν and $2-\nu$, we must now use the orthotropic coefficients β_1 and β_2 (respectively) defined in (2.23) in the same way as in Sect. 2.1.3 (their definitions are repeated at the end of this subsection for convenience).

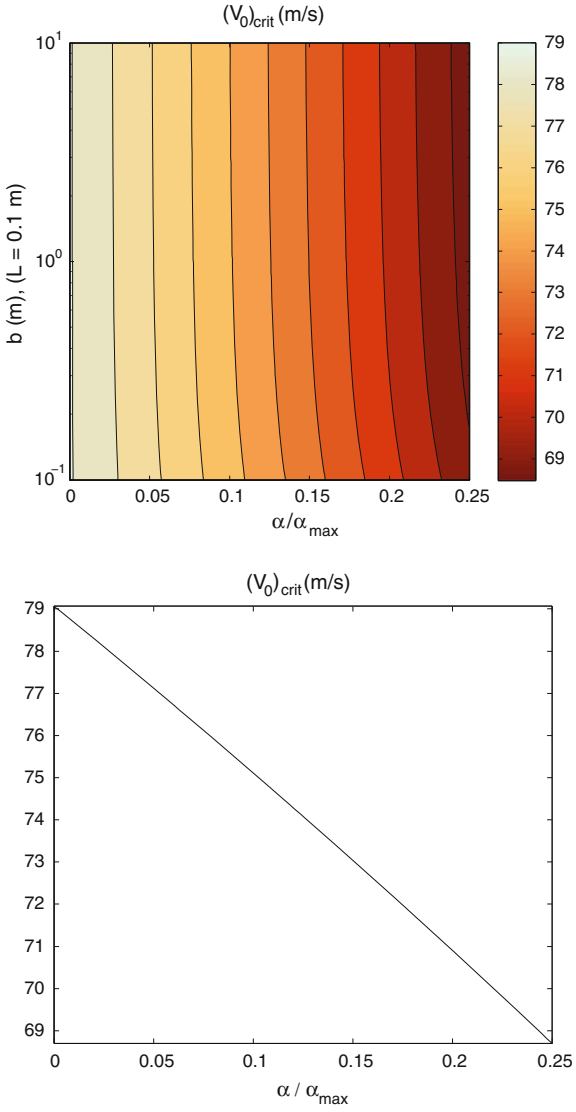

Fig. 4.3 *Top* Critical plate velocity $(V_0)_{\text{crit}}$ with respect to the tension profile skew parameter α and plate half-width b. Note the logarithmic scale for b. The plate length is constant ($\ell = 0.1\,\text{m}$). *Bottom* The critical velocity plotted with respect to the tension profile skew parameter ($\ell = 0.1\,\text{m}$, $2b = 1\,\text{m}$). (Reproduced from Banichuk et al. 2013)

In Sect. 2.2, the in-plane tension field for an orthotropic plate in the case of a linear tension distribution was solved with the help of the Airy stress function. See Eqs. (2.50) and (2.51).

To determine the minimal eigenvalue λ (4.39), and the corresponding eigenfunction, of the problem (4.44) with boundary conditions (4.18–4.20) (modified for the orthotropic case as explained), we apply the representation (4.37). By using the dimensionless quantities η and μ in (4.38), the free-of-traction boundary conditions

(4.19) and (4.20), with the relations (4.39), (4.44) and (4.37), we obtain the eigenvalue problem for the orthotropic case:

$$\mu^4 H_2 \frac{\mathrm{d}^4 f}{\mathrm{d}\eta^4} - 2\mu^2 H_3 \frac{\mathrm{d}^2 f}{\mathrm{d}\eta^2} + (H_1 - \lambda - \bar{\alpha}\eta)\, f = 0\,, \quad -1 < \eta < 1\,, \tag{4.45}$$

$$\mu^2 \frac{\mathrm{d}^2 f}{\mathrm{d}\eta^2} - \beta_1 f = 0\,, \quad \eta = \pm 1 \quad \text{and} \tag{4.46}$$

$$\mu^2 \frac{\mathrm{d}^3 f}{\mathrm{d}\eta^3} - \beta_2 \frac{\mathrm{d} f}{\mathrm{d}\eta} = 0\,, \quad \eta = \pm 1. \tag{4.47}$$

In (4.45), the dimensionless tension profile skew parameter is defined as

$$\bar{\alpha} = \frac{b\ell^2}{\pi^2 D_0}\alpha = \frac{b^3\mu^2}{D_0}\alpha \tag{4.48}$$

and the H_j are the dimensionless bending rigidities defined by (3.91), Sect. 3.5, repeated here for convenience:

$$H_1 = \frac{D_1}{D_0}\,, \qquad H_2 = \frac{D_2}{D_0}\,, \qquad H_3 = \frac{D_3}{D_0}.$$

As before, D_0 is the normalization factor for the bending rigidities and can be chosen arbitrarily. A convenient choice is $D_0 = D_1$. In (4.46) and (4.47), the β_j are defined in (2.23) in Sect. 2.1.3, also repeated here for convenience:

$$\beta_1 = \nu_{12}\,,$$

$$\beta_2 = \nu_{12} + \frac{4\,G_{12}}{E_2}\,(1 - \nu_{12}\nu_{21})\,.$$

Again, we have a linear eigenvalue problem with polynomial coefficients.

For the rest of this chapter, we will concentrate on the isotropic case.

4.3.2 Numerical Analysis

We will proceed with a numerical solution of the eigenvalue problem for the isotropic elastic plate. Finite differences will be used, with virtual points added to the ends of the domain to enforce the boundary conditions.

As the considered problem is linear in f, the discretization will lead to a standard discrete linear eigenvalue problem representing (4.40):

$$\mathbf{A}\mathbf{f} = \lambda \mathbf{f}. \tag{4.49}$$

Equation (4.49) does not yet include the boundary conditions (4.42)–(4.43). Because the boundary conditions are homogeneous, it is possible to add them to the discrete system by rewriting the original discrete problem (4.49) as a generalized linear eigenvalue problem,

$$\mathbf{A}\mathbf{f} = \lambda \mathbf{B}\mathbf{f} \ , \tag{4.50}$$

where $\mathbf{B}$ is an identity matrix with the first two and last two rows zeroed out. In (4.50), the first two and the last two rows of A contain discrete representations of the boundary conditions (4.42)–(4.43).

The details are as follows. Equations (4.40)–(4.43) are to be discretized. The standard central difference formulas, of second-order asymptotic accuracy, for the first four derivatives on a uniform grid are

$$\frac{\partial f_j}{\partial \eta} \approx \frac{f_{j+1} - f_{j-1}}{2\,(\Delta\eta)} \ , \tag{4.51}$$

$$\frac{\partial^2 f_j}{\partial \eta^2} \approx \frac{f_{j+1} - 2\,f_j + f_{j-1}}{(\Delta\eta)^2} \ , \tag{4.52}$$

$$\frac{\partial^3 f_j}{\partial \eta^3} \approx \frac{f_{j+2} - 2\,f_{j+1} + 2\,f_{j-1} - f_{j-2}}{2\,(\Delta\eta)^3} \ , \tag{4.53}$$

$$\frac{\partial^4 f_j}{\partial \eta^4} \approx \frac{f_{j+2} - 4\,f_{j+1} + 6\,f_j - 4\,f_{j-1} + f_{j-2}}{(\Delta\eta)^4} \ , \tag{4.54}$$

where $f \equiv f(x)$ is the function to be differentiated, $f_j \equiv f(\eta_j)$, and $\Delta\eta$ is the grid spacing.

When the derivatives in (4.40) are replaced by the discrete approximations (4.52) and (4.54) for each grid point η_j, we obtain the discrete equation system for the interior of the domain. The $\bar{\alpha}\eta$ term is handled by substituting in the coordinate of the jth grid point, $\eta_j = j\,(\Delta\eta)$. Then the discrete equations are collected into matrix form, and the $\lambda\mathbf{f}$ term is moved to the right-hand side.

The boundary conditions (4.42)–(4.43) are then handled by adding two virtual points at each end of the domain. Applying (4.51)–(4.54) to the boundary conditions produces discrete equations connecting the function values at the virtual points to those inside the domain.

If we number the points starting at 1 at the first (outermost) virtual point at the left end of the domain, the final left-hand side matrix becomes

$$\mathbf{A} \equiv \mathbf{A}_4 + \mathbf{A}_2 + \mathbf{A}_0 + \mathbf{L}_1 + \mathbf{L}_2 + \mathbf{L}_3 + \mathbf{L}_4 \ ,$$

where the terms $\mathbf{A}_m$ correspond to Eq. (4.40), and are given by

$$\mathbf{A}_4 \equiv \frac{\mu^4}{(\Delta\eta)^4}\begin{bmatrix} 0 & \dots & & & & \dots & 0 \\ 0 & \dots & & & & \dots & 0 \\ 1 & -4 & 6 & -4 & 1 & & \\ & \ddots & \ddots & \ddots & \ddots & \ddots & \\ & & 1 & -4 & 6 & -4 & 1 \\ 0 & \dots & & & & \dots & 0 \\ 0 & \dots & & & & \dots & 0 \end{bmatrix},$$

$$\mathbf{A}_2 \equiv -\frac{2\mu^2}{(\Delta\eta)^2}\begin{bmatrix} 0 & \dots & & & & \dots & 0 \\ 0 & \dots & & & & \dots & 0 \\ 0 & 1 & -2 & 1 & & & \\ & & \ddots & \ddots & \ddots & & \\ & & & 1 & -2 & 1 & 0 \\ 0 & \dots & & & & \dots & 0 \\ 0 & \dots & & & & \dots & 0 \end{bmatrix},$$

$$\mathbf{A}_0 \equiv \begin{bmatrix} 0 & \dots & & & \dots & 0 \\ 0 & 0 & \dots & & \dots & 0 \\ 0 & 0 & a_k & & \dots & 0 \\ & & & \ddots & & \\ 0 & \dots & & a_k & 0 & 0 \\ 0 & \dots & & \dots & 0 & 0 \\ 0 & \dots & & & \dots & 0 \end{bmatrix},$$

where

$$a_k \equiv 1 + \bar{\alpha}\ [-1 + (k-3)\,(\Delta\eta)]$$

and k denotes the row number of the matrix $\mathbf{A}_0$. The first contribution in $\mathbf{A}_0$ is $1 - \bar{\alpha}$ (on row 3, corresponding to the point at $\eta = -1$), and the last is $1 + \bar{\alpha}$ (third last row, corresponding to $\eta = +1$).

Empty entries in the matrices denote zeroes; some zeroes are displayed explicitly to show more clearly where the nonzero entries belong.

The terms $\mathbf{L}_m$ correspond to the boundary conditions (4.42)–(4.43), and are given by

$$\mathbf{L}_1 \equiv \begin{bmatrix} 0 & \dots & & & \dots & 0 \\ 0 & \mu^2/(\Delta\eta)^2 & -2\mu^2/(\Delta\eta)^2 - \nu & \mu^2/(\Delta\eta)^2 & \dots & 0 \\ 0 & \dots & \dots & \dots & \dots & 0 \\ 0 & \dots & \dots & \dots & \dots & 0 \\ 0 & \dots & \dots & \dots & \dots & 0 \\ 0 & \dots & & & \dots & 0 \\ 0 & \dots & & & \dots & 0 \end{bmatrix},$$

$$\mathbf{L}_2 \equiv \begin{bmatrix} -\mu^2/[2(\Delta\eta)^3] & \chi & 0 & -\chi & \mu^2/[2(\Delta\eta)^3] & 0 \dots 0 \\ 0 & \dots & & & & \dots 0 \\ 0 & \dots & & & & \dots 0 \\ 0 & \dots & & & & \dots 0 \\ 0 & \dots & & & & \dots 0 \\ 0 & \dots & & & & \dots 0 \\ 0 & \dots & & & & \dots 0 \end{bmatrix},$$

$$\mathbf{L}_3 \equiv \begin{bmatrix} 0 \dots & & & & \dots & 0 \\ 0 \dots & & & & \dots & 0 \\ 0 \dots & \dots & \dots & \dots & \dots & 0 \\ 0 \dots & \dots & \dots & \dots & \dots & 0 \\ 0 \dots & \dots & \dots & \dots & \dots & 0 \\ 0 \dots & \mu^2/(\Delta\eta)^2 & -2\mu^2/(\Delta\eta)^2 - \nu & \mu^2/(\Delta\eta)^2 & 0 \\ 0 \dots & & & & \dots & 0 \end{bmatrix},$$

$$\mathbf{L}_4 \equiv \begin{bmatrix} 0 \dots & & & & \dots & 0 \\ 0 \dots & & & & \dots & 0 \\ 0 \dots & & & & \dots & 0 \\ 0 \dots & & & & \dots & 0 \\ 0 \dots & & & & \dots & 0 \\ 0 \dots & & & & \dots & 0 \\ 0 \dots & -\mu^2/[2(\Delta\eta)^3] & \chi & 0 & -\chi & \mu^2/[2(\Delta\eta)^3] \end{bmatrix},$$

where in $\mathbf{L}_2$ and $\mathbf{L}_4$ we use the notation

$$\chi \equiv \mu^2/(\Delta\eta)^3 + (2-\nu)/[2(\Delta\eta)].$$

The matrices $\mathbf{L}_1$ and $\mathbf{L}_3$ correspond to the boundary condition (4.42) at the left and right endpoints of the domain, respectively, while $\mathbf{L}_2$ and $\mathbf{L}_4$ correspond to (4.43).

Finally, the discrete problem (4.50) is completed by defining

$$\mathbf{B} \equiv \begin{bmatrix} 0 \dots & & & \dots 0 \\ 0 \;\; 0 \;\; \dots & & & \dots 0 \\ 0 \;\; 0 \;\; 1 & & & \dots 0 \\ & \ddots & & \\ 0 \dots & & 1 \;\; 0 \;\; 0 & \\ 0 \dots & & \dots \;\; 0 \;\; 0 & \\ 0 \dots & & & \dots 0 \end{bmatrix},$$

which enforces the homogeneous boundary conditions (4.42)–(4.43), represented by the first two and last two rows of the discrete equation system.

In order to solve the original problem, we compute the solution of (4.50), discard eigenvalues of infinite magnitude, which result from our way of handling the

boundary conditions, and then extract the smallest eigenvalue λ and its corresponding eigenvector $\mathbf{f}$. The first two and last two components of the eigenvector are discarded, because they represent the function values at virtual points that were generated from the boundary conditions. Finally, the buckling mode (divergence mode) $W(x, y)$ is constructed using the equation

$$W(x, y) = f\left(\frac{\pi y}{\ell}\right) \sin\left(\frac{\pi x}{\ell}\right).$$

Below, numerical results are shown for some practically interesting choices of problem parameters. The physical parameters used in the examples are presented in Table 4.1. These parameter values approximately correspond to some paper materials, within the limitations of the isotropic model.

Various values of the Poisson ratio ν and the tension profile skew parameter $\tilde{\alpha}$ are used in the examples. For the Poisson ratio, the values 0, 0.1, 0.3 and 0.5 are used. The values of $\alpha/\alpha_{\max}$ (or $\tilde{\alpha}/\tilde{\alpha}_{\max}$) are 0, 10^{-6}, 10^{-4} and 10^{-2}, where $\alpha_{\max}$ corresponds to the upper limit imposed by the constraint (4.36), $\alpha < T_0/b$. Note that $\tilde{\alpha}_{\max}$ depends on ν, via D. In Table 4.2, critical divergence velocities are presented for these cases. The analytical solution for $\tilde{\alpha} = 0$ for the same geometric and material parameters (see (3.39), (3.54–3.56)) matches the values in the first column of the table.

The results for the transverse displacement are shown in Figs. 4.4, 4.5 and 4.6. In each figure, ν is fixed. Figure 4.4 is divided into two parts. Both parts of the figure are further divided into four subfigures. Each of these four subfigures shows the results for a different value of the skew parameter $\tilde{\alpha}$. In the upper four subfigures, $f(\eta)$ is plotted, showing a slice of the out-of-plane displacement from one free edge to the other at $x = \ell/2$. Tension increases toward positive η. The total out-of-plane displacement in the whole domain Ω, from Sequation $W = f(\pi y/\ell) \sin(\pi x/\ell)$, is shown in the lower four subfigures. Note the orientation of the axes. In Figs. 4.5 and 4.6,

Table 4.1 Physical parameters used in the numerical examples.

T_0 (tension at $y = 0$)	m	ℓ	$2b$	h	E
500 N/m	0.08 kg/m^2	0.1 m	1 m	10^{-4} m	10^9 N/m^2

Table 4.2 Critical divergence velocities V_0^{div} for example cases

ν	$\tilde{\alpha}$			
	0	$10^{-6}\tilde{\alpha}_{\max}$	$10^{-4}\tilde{\alpha}_{\max}$	$10^{-2}\tilde{\alpha}_{\max}$
0	79.0634	79.0634	79.0605	78.6892
0.1	79.0635	79.0635	79.0605	78.6886
0.3	79.0640	79.0640	79.0609	78.6876
0.5	79.0652	79.0652	79.0618	78.6870

Note that $\tilde{\alpha}_{\max}$ is different for each value of ν (Banichuk et al. 2013)

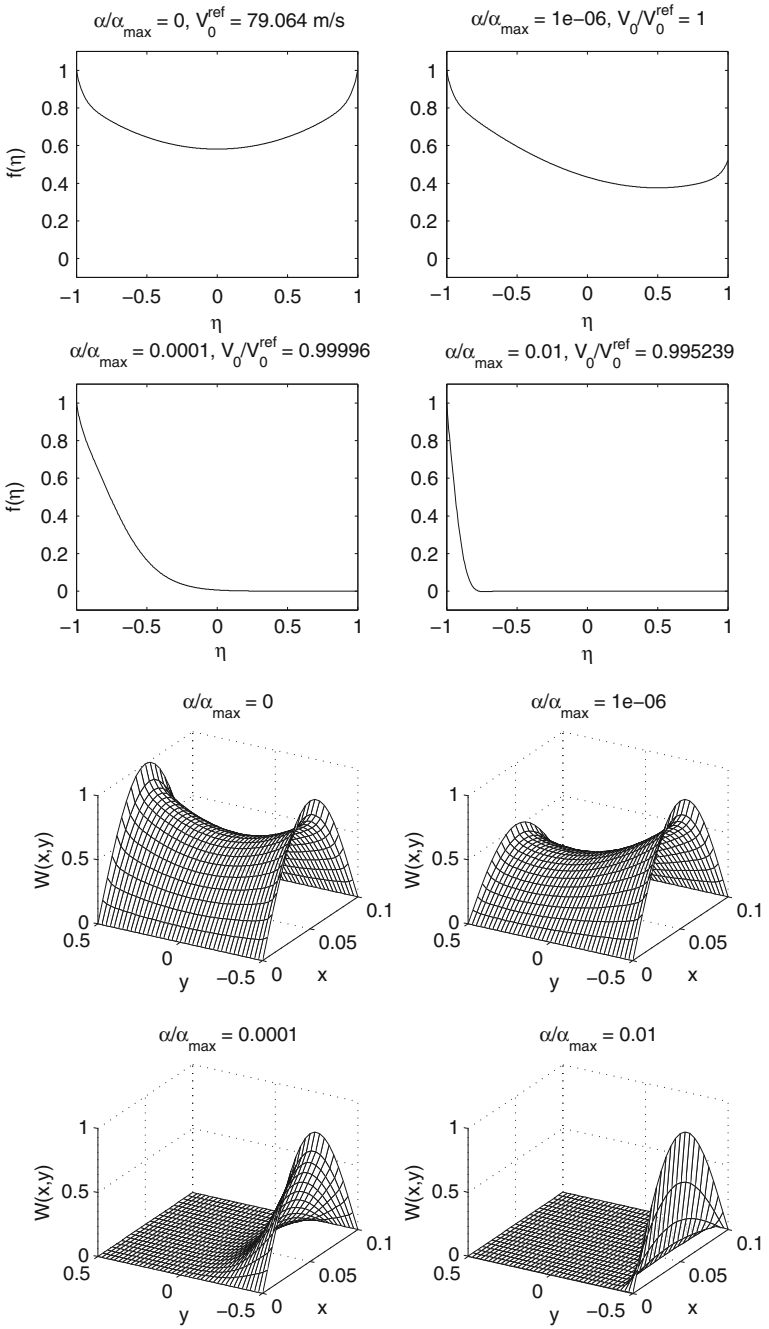

Fig. 4.4 Out-of-plane displacement of an axially travelling pinned-free plate with dimensions $\ell = 0.1\,\text{m}$ (length), $2b = 1\,\text{m}$ (width), $h = 10^{-4}\,\text{m}$ (thickness). Poisson ratio $\nu = 0.3$. Tension profile skew parameter $\alpha/\alpha_{\max} = 0,\ 10^{-6},\ 10^{-4},\ 10^{-2}$. (Reproduced from Banichuk et al. 2013)

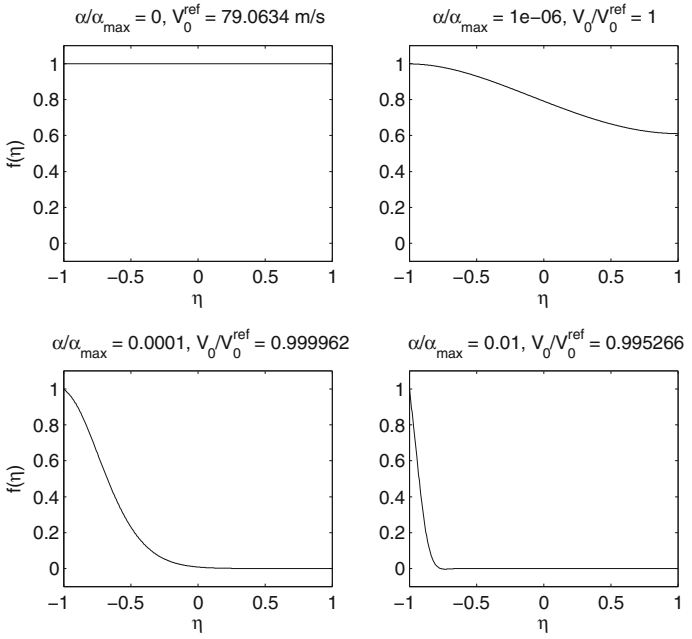

Fig. 4.5 Out-of-plane displacement of an axially travelling pinned-free plate at $x = \ell/2$ with dimensions $\ell = 0.1$ m (length), $2b = 1$ m (width), $h = 10^{-4}$ m (thickness). Poisson ratio $\nu = 0$. Tension profile skew parameter $\alpha/\alpha_{\max} = 0,\ 10^{-6},\ 10^{-4},\ 10^{-2}$. (Reproduced from Banichuk et al. 2013)

the four subfigures show the slices of the out-of-plane displacement at $x = \ell/2$ for the limit cases $\nu = 0$ and $\nu = 0.5$, in analogous order.

From Figs. 4.3, 4.4, 4.5 and 4.6 and Table 4.2, three conclusions are apparent. First, it is seen that inhomogeneities in the tension profile may significantly decrease the critical velocities. Up to a 20 % tension inhomogeneity between the midpoint and edges causes a decrease in critical velocity of 10 %. It is also seen that a wider plate is more sensitive to tension inhomogeneities. Secondly, by comparing Figs. 4.4, 4.5 and 4.6, it is observed that materials with a larger Poisson ratio tend to exhibit a higher degree of sensitivity to inhomogeneities in the tension profile.

Finally, we see that even for the smallest inhomogeneity in the examples (one part in 10^6), for the problem parameters considered the buckling mode (divergence mode) changes completely. Thus, from a practical point of view, although studies of the homogeneous tension case can predict the critical velocity relatively accurately, the obtained results indicate that if one wishes to predict the divergence shape, even a small inhomogeneity in the tension must be accounted for.

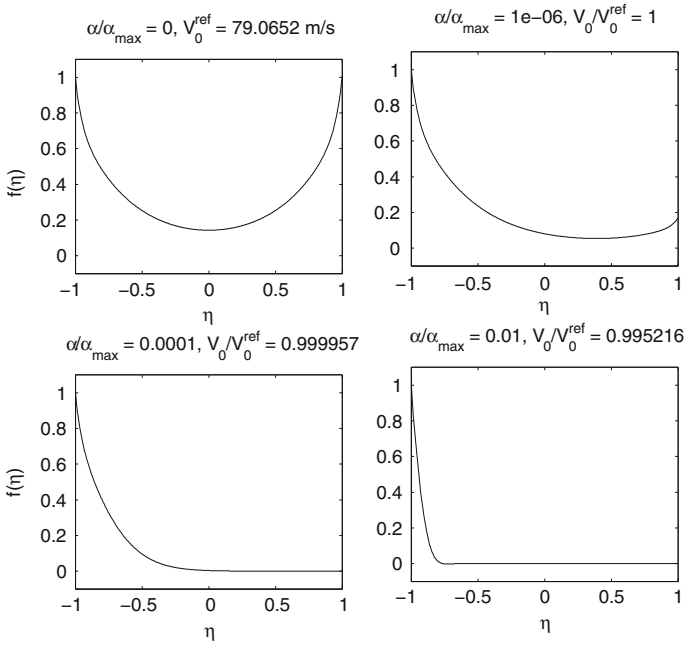

Fig. 4.6 Out-of-plane displacement of an axially travelling pinned-free plate at $x = \ell/2$ with dimensions $\ell = 0.1\,\text{m}$ (length), $2b = 1\,\text{m}$ (width), $h = 10^{-4}\,\text{m}$ (thickness). Poisson ratio $\nu = 0.5$. Tension profile skew parameter $\alpha/\alpha_{\max} = 0,\ 10^{-6},\ 10^{-4},\ 10^{-2}$. (Reproduced from Banichuk et al. 2013)

The sensitivity to the inhomogeneity is affected also by the tension at midpoint T_0. The higher the tension, the more sensitive the system is to small inhomogeneities. This effect is shown in Fig. 4.7. The subfigure on the bottom left of this figure corresponds to the subfigure at the top right of Fig. 4.4. We see that with $\nu = 0.3$, $\tilde{\alpha} = 10^{-6}\tilde{\alpha}_{\max}$, and the values of the other parameters fixed to those given at the beginning of this section, the sensitivity is very high already at $T_0 = 500\,\text{N/m}$, which is realistic in the application of paper production.

It should be noted that as far as geometric parameters are concerned, the divergence shape is a function of not only the aspect ratio $\ell/2b$, but also the overall scale. Even for the same aspect ratio, scaling ℓ (and also b to keep the same aspect ratio) changes the divergence shape. This effect occurs even if h is scaled by the same amount as ℓ and b. Thus, it should be emphasized that the results in Figs. 4.4, 4.5, 4.6 and 4.7 only represent the specific case of plates with the dimensions $\ell \times 2b \times h = 0.1\,\text{m} \times 1\,\text{m} \times 10^{-4}\,\text{m}$.

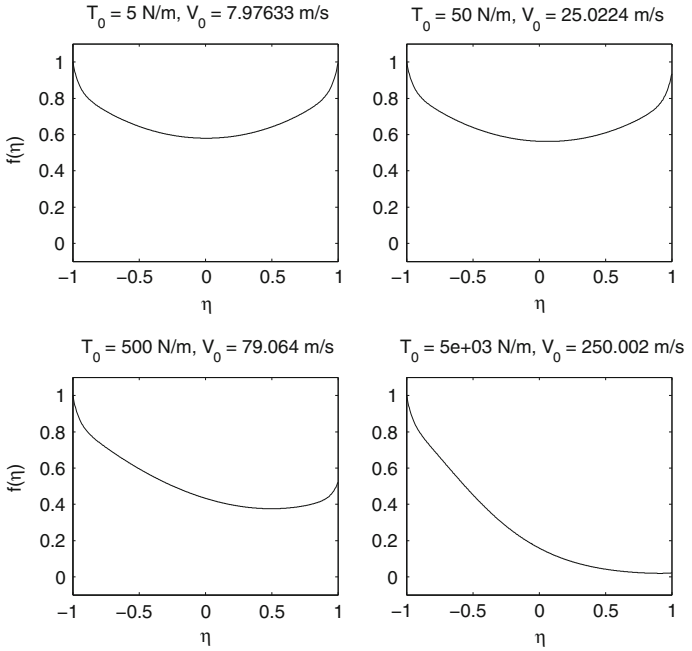

Fig. 4.7 Out-of-plane displacement of an axially travelling pinned-free plate at $x = \ell/2$ with dimensions $\ell = 0.1$ m (length), $2b = 1$ m (width), $h = 10^{-4}$ m (thickness). Poisson ratio $\nu = 0.3$, tension profile skew parameter $\alpha/\alpha_{\max} = 10^{-6}$. Midpoint tension $T_0 = 5,\ 50{,}500$ and $5{,}000$ N/m. (Reproduced from Banichuk et al. 2013)

References

Banichuk N, Jeronen J, Neittaanmäki P, Saksa T, Tuovinen T (2013) Theoretical study on travelling web dynamics and instability under non-homogeneous tension. Int J Mech Sci 66C:132–140. http://dx.doi.org/10.1016/j.ijmecsci.2012.10.014

Bolotin VV (1963) Nonconservative Problems of the theory of elastic stability. Pergamon Press, New York

Chang YB, Moretti PM (1991) Interaction of fluttering webs with surrounding air. TAPPI J 74(3):231–236

Timoshenko SP, Woinowsky-Krieger S (1959) Theory of plates and shells, 2nd edn. McGraw-Hill, New York, ISBN 0-07-085820-9